Advances in Computer, Signals and Systems (2026)
Clausius Scientific Press, Canada

DOI: 10.23977/acss.2026.100102
ISSN 2371-8838 Vol. 10 Num. 1

Two general filters for image enhancement and their applications for images acquired from a transmission electron microscope and a fluorescence microscope

Jiangqi Luo[1,a], Ling Zhang[2,b,*], Yingcheng Lin[2,c,*],Ye Wu[3,4,d,*]

[1]Qigongxi Industrial Design Center, Qinhuai District, Nanjing, 211000, China
[2]College of Microelectronics and Communication Engineering, Chongqing University, Chongqing, 400044, China
[3]School of Electrical and Information Engineering, Hunan Institute of Technology, Hengyang, 421002, China
[4]School of Electrical and Automation Engineering, Nanjing Normal University, Nanjing, 210046, China
[a]75733145@qq.com, [b]zhangling1993@cqu.edu.cn, [c]linyc@cqu.edu.cn, [d]wooye@163.com
**Corresponding authors*

Keywords: Image enhancement; matched filters; low-light images; transmission electron microscope; fluorescence microscope; near infrared imaging

Abstract: Image enhancement is important in image processing. It can improve image contrast, highlight details and suppress noise. This work proposes two general filters based on mathematical functions for the image enhancement. The first filter was designed using logarithmic, anti-trigonometric and hypotenuse functions. The second filter was designed using trigonometric and anti-trigonometric functions. These two filters can be used for processing the images acquired from fluorescence microscope and transmission electron microscope. We also use them to process images containing nesting structures, weak-light images and images with high degradation by the Gaussian noise. They are effective to achieve better enhancement of the images.

1. Introduction

Image enhancement plays a crucial role in image processing, as it can significantly improve image quality. It is widely used as a preprocessing step for target recognition, target tracking, and image fusion [1]. Over the past decades, numerous image enhancement techniques have been developed, including histogram equalization (HE) [2], wavelet transform–based methods [3–5], and Retinex theory–based approaches [6–9].

Histogram equalization is a commonly used technique that effectively improves image contrast; however, it may lead to information loss and the disappearance of small-scale objects. Wavelet transform–based enhancement methods decompose an image into low-frequency and high-frequency components, allowing image details to be emphasized by enhancing different frequency bands. Nevertheless, these methods tend to amplify noise. Retinex-based methods, inspired by the principles

of retinal imaging, aim to simulate the human visual system, but they often suffer from local detail loss and inevitable image distortion. Another class of image enhancement methods employs fuzzy logic techniques [10–13]. Since images inherently exhibit fuzziness, fuzzy theory can be applied to better represent image information. However, traditional fuzzy-based enhancement algorithms are computationally intensive, fail to incorporate multi-level contour information, and often rely on empirically chosen parameters that do not guarantee optimal performance.

In this work, we postulate that the appropriate selection of mathematical functions for filter construction is the key to achieving desired frequency characteristics. By combining simple yet general mathematical functions, effective filters can be designed. Through carefully constructed special functions, image signals with different frequency components can be selectively enhanced, thereby highlighting fine image details.

Based on this concept, we designed two image enhancement filters using special functions. These filters were applied to images acquired from fluorescence microscopy and transmission electron microscopy (TEM). In life sciences, fluorescence microscopy is widely used to investigate the absorption, transport, distribution, and localization of chemical substances within cells or tissues, and the resulting images contain rich structural information. In contrast, TEM images often exhibit substantial noise due to electron beam distortion and the extremely small size of the samples. Enhancing images from both imaging modalities is therefore of critical importance.

The remainder of this paper is organized as follows. Section 2 introduces the proposed framework. Section 3 presents the experimental results and discussion, focusing on fluorescence microscopy and TEM images. We further explore the application of the proposed filters to images with nested structures, images degraded by Gaussian noise, low-light images, and images containing objects of varying widths. Images captured under low-light conditions are typically dark and noisy, which poses significant challenges for subsequent computer vision tasks such as tracking, detection, and recognition. High-quality, clear images are essential for accurate analysis, making low-light image enhancement particularly important. Notably, our results demonstrate that the proposed filters are effective in enhancing weak-light images. Finally, the main conclusions and future perspectives are summarized in the last section.

2. Method

This section presents the detail of two frameworks based on special functions. The proposed framework is explained in two phases. Firstly, we pre-process the images, including conversion to gray-scale, resizing images and storing the image data as doubles. Then, we processed the images with special functions to enhance the images.

2.1. The log-hypot-log-sech filter

The pre-processing included reading image, converting to gray-image, resizing image and converting data to double. After pre-processing, we have generated an array of matrix uu(m,n). We perform wavelet packet transformation on uu(m,n). In other words, we generate a wavelet packet tree T associated with the wavelet packet decomposition of the matrix uu(m,n), at level N, with the specified wavelet. We reconstruct the coefficient from one specific node of the wavelet packet tree T and generate a new coefficient A. With this new coefficient A, we can use the combination of logarithmic functions, hypotenuse formulas, and hyperbolic functions to get the new pixel values.

The detailed algorithm is shown in Algorithm 1.

Algorithm 1: The algorithm of the log-hypot-log-sech filter for the image enhancement
1: Reading the image in JPG format 2: Converting the image into a gray image

3: The image is resized to be 2660 2660
4: Converting the pixels value to double
5: Generating a wavelet packet tree T
6: Reconstructing the coefficient from one specific node of the wavelet packet tree T and generating a new coefficient A
7: Defining the parameters h and w representing size of the image
8: for each iteration m=3 to h-1 do
9: for each iteration n=3 to w-1 do
10: Defining all the constants, defining r is the pixel value associated with A and calculating the functions:

$r_1 = \mathrm{a}_1 \cos(\mathrm{r}) + \mathrm{a}_2 \sin(r)$

$r_2 = \log(r_1 \times a_3 + a_4)$

$r_3 = a_5 \times hypot(r_1, r_2)$

$z = \log[\frac{\mathrm{a}_6 \times \mathrm{sech}(r_3 + a_7)}{2a}]$

$u(m,n) = z^{a_8}$

end for

end for

Here, a_1, a_2, a_3, a_4, a_5, a_6, a_7 and a_8 are constants. r is the pixel value associated with A. u(m,n) is the final pixel value of the algorithm, which can be used to generate an output image.

11: Showing the processed image

2.2. The sech-acosh-cosh filter

We first read the image in JPG format, convert it into a gray image and resize the image into 2660×2660. We can generate a matrix tt(m,n) representing the image. After we run the wavelet decomposition of tt(m,n) at certain level using the specific wavelet, we can acquire the wavelet decomposition vector C. We modify C using the functions of "sech, acosh, and cosh" in order to generate a new coefficient C_4. We perform the inverse of the wavelet transform of C_4 and generate new pixel values of *qq(m,n)*, which will be used for constructing the new image.

The detailed algorithm is shown in Algorithm 2.

Algorithm 2: The algorithm of the sech-acosh-cosh filter for the image enhancement

1: Reading the image in JPG format

2: Converting the image into a gray image

3: The image is resized to be 4000× 4000

4: Generating a matrix tt(m,n) representing the image.

5: Running the wavelet decomposition of tt(m,n) at certain level using the specific wavelet and acquiring the wavelet decomposition vector C.

6. Modifying C using the following equations:

$$C_1 = \mathrm{sech}(C)$$

$$z = \mathrm{acosh}\left[\frac{\mathrm{b}_1 \times \cosh(\mathrm{C} + b_2)}{\mathrm{C}_1}\right]$$

$$C_3 = \mathrm{real}(\mathrm{C}_1)$$

$$C_4 = \mathrm{C}_3{}^{b_3}$$

7. Performing the inverse of the wavelet transform of C_4 and generate new pixel values of qq(m,n)

(Here, “real” means we only use the real part and dump the imaginary part. b_1, b_2 and b_3 are constants)

8. Constructing the new image based on qq(m,n)

3. Results and discussion

3.1. Processing the image acquired from the fluorescence microscope

Figure 1a is a fungal image called as YW17-Fungal. Figure 1b, 1c are the images processed by the two filters. Fig.1d is the image processed by the Sobel operator. These images indicate that our filters are good for image enhancement. They can preserve more details of the original figures comparing to the Sobel operator. They can preserve the size and position of the information as clearly indicated in the original image. It should be noted that the Sobel operator is difficult to achieve the enhancement of images acquired from the fluorescence microscope (Figure 1d).

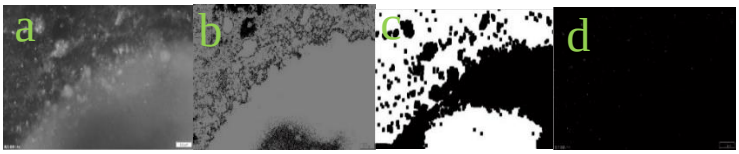

Figure 1: (a) An image called as YW17-Fungal. (b) Processed by the log-hypot-log-sech filter. (c) Processed by the sech-acosh-cosh filter. (d) Processed by the Sobel operator.

3.2. Processing the image acquired from transmission electron microscope

In order to explore the processing effect of our designed filters with the transmission electron microscope, we use the image TEM1 (Figure 2a). We also compared the processing with the Sobel operator. Compared with the image processed by the Sobel operator (Figure 2d), those images (Figures 2b, 2c) acquired from our developed filters can show more details of the nanoparticles in Figure 2a. They can clearly show the size and position of the nanoparticles. The image noise is also removed.

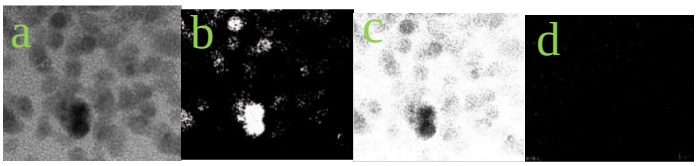

Figure 2: (a) An image called as TEM1. (b) Processed by the log-hypot-log-sech filter. (c) Processed by the sech-acosh-cosh filter. (d) Processed by the Sobel operator.

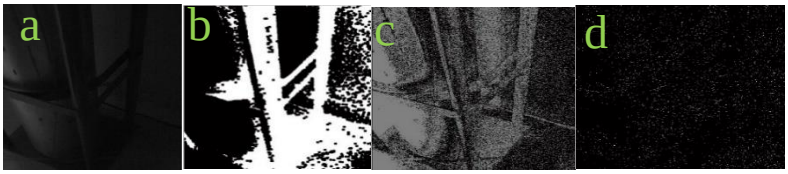

Figure 3: (a) An image called as Bottle. (b) Processed by the log-hypot-log-sech filter. (c) Processed by the sech-acosh-cosh filter. (d) Processed by the Sobel operator.

3.3. Processing the weak-light images

Images captured under weak-light conditions have poor contrast, blurred content and missing

details. It is important to enhance the brightness and contrast of the image. We used a weak-light image called as Bottle for processing (Figure 3a). The images processed using our filters can enhance the brightness and contrast (see Figures 3b, 3c). It can highlight the shape of the bottle and the outline of shelf with clear edges. When it was processed by the Sobel operator, it returns barely nothing but the noise (Figure 3d).

3.4. Processing the nesting images

We have a series of nested images, as shown in Figures 4a, 5a, 6a. The three different images are called as Arrow, Rectangle and Orange. For comparing study, we also use the Sobel operator to process these images. The results are shown in Figures 4-6. It clearly showed that our two filters can generate clearer edge, more image details. Moreover, the contrast with the background is sharp.

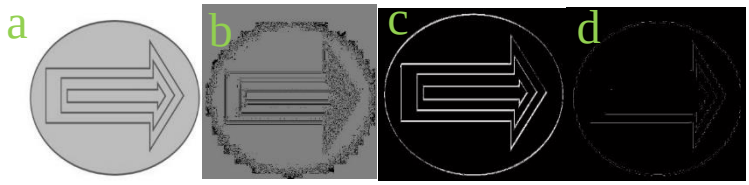

Figure 4: (a) An image called as Arrow. (b) Processed by the log-hypot-log-sech filter. (c) Processed by the sech-acosh-cosh filter. (d) Processed by the Sobel operator.

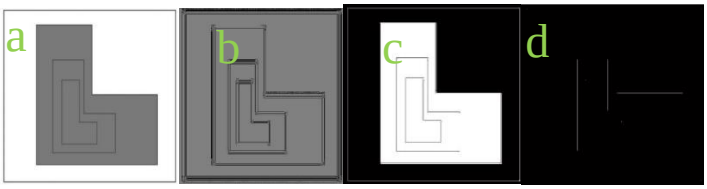

Figure 5: (a) An image called as Rectangle. (b) Processed by the log-hypot-log-sech filter. (c) Processed by the sech-acosh-cosh filter. (d) Processed by the Sobel operator.

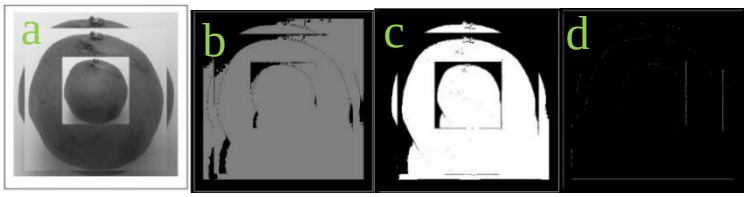

Figure 6: (a) An image called as Orange. (b) Processed by the log-hypot-log-sech filter. (c) Processed by the sech-acosh-cosh filter. (d) Processed by the Sobel operator.

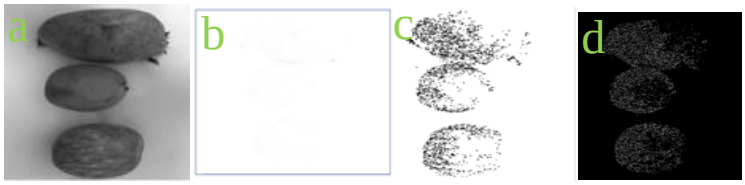

Figure 7: (a) An image called as Fruit. (b) Degraded by the Gaussian noise with a density of 0.9. (c) Processed by the log-hypot-log-sech filter. (d) Processed by the sech-acosh-cosh filter.

3.5. Processing the images with high degradation by the Gaussian noise

Enhancing the image with high degradation has become an indispensable technical step in image

processing. In order to show that our filters can be useful, we add a Gaussian noise to an image called Fruit. The noise density is 0.9. As shown in Figure 7, our developed filters can delete the Gaussian noise and recover the shape of the object.

3.6. Processing images containing objects of different width

We draw an image called as “Array”, which shows nested objects of different width. We process it using our developed filters (Figure 8b and Figure 8c). Clear edge can be extracted.

We also process it using several well-known filters, such as filter based on the watershed algorithm (Figure 8d), the filter based on Gabor wavelets (Figure 8e) and the matched filter (Figure 8f). These images acquired show some drawbacks. The nested objects acquired from the filter based on watershed algorithm and the filter based on the Gabor wavelets are distorted. The smallest objects are missing when it is processed by the matched filter.

Images acquired from fluorescence microscopy and transmission electron microscopy are often susceptible to degradation caused by low contrast, image blurring, and a low signal-to-noise ratio. We demonstrate that the filters developed in this work effectively enhance images obtained under such adverse conditions. Specifically, the proposed filters preserve most of the structural and profile information present in the original images while significantly improving contrast and suppressing noise, thereby facilitating clearer visual interpretation by the human eye.

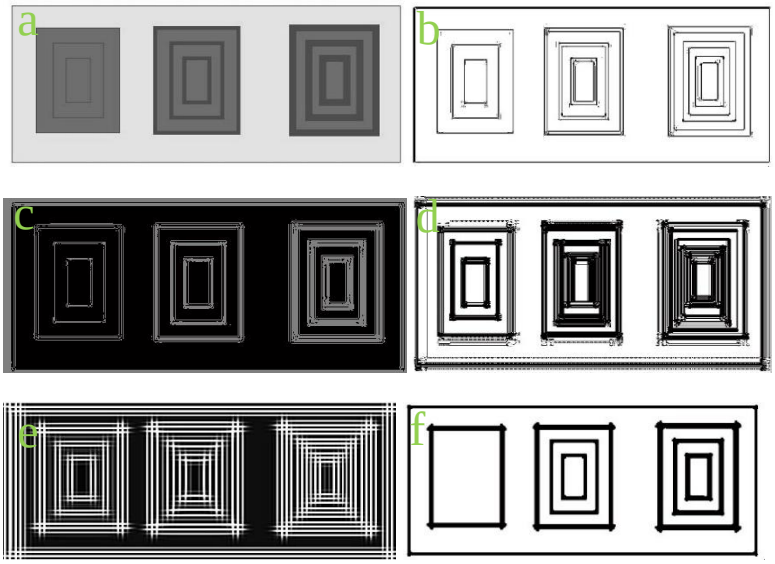

Figure 8. (a) An image called as Array. (b) Processed by the log-hypot-log-sech filter. (c) Processed by the sech-acosh-cosh filter. (d) Processed by the filter based on watershed algorithm. (e) Processed by the filter based on Gabor wavelets. (f) Processed by the matched filter.

Images captured under weak-light conditions typically suffer from poor quality, including low contrast, severe noise, and blurred edges and textures. Our filters effectively enhance image brightness and contrast under low-light conditions while extracting salient image contours. In addition, the proposed filters are capable of processing images with extremely high levels of degradation noise. To evaluate robustness, we artificially added noise with a density of 0.9 to test images; the filtering results indicate that our method maintains satisfactory performance even under such severe noise conditions.

The proposed functional forms are highly flexible and can be readily modified to accommodate the processing requirements of diverse image types. Future work will focus on adapting these filters to meet the intensive computational demands of computer systems [14], the Internet of Things [15],

and sensor and network-based platforms [16–20]. Moreover, computational efficiency, entropy analysis, and integration with advanced system frameworks were not considered in the present study and will be addressed in future investigations [21–27]. Another promising research direction involves combining the proposed filtering approach with nanoparticle- and small-molecule-based imaging techniques to further reduce image noise at the acquisition stage [28–37].

4. Conclusions

Image enhancement is important in digital image processing. It can adjust image brightness, enhance image contrast, remove image noise, and extract image information. In this work, two filters based on special functions are designed. They are useful for processing the images in a series of nested set, the image acquired from the fluorescence microscope, the image acquired from transmission electron microscope, the weak-light image, the image with high degradation by the Gaussian noise and the image containing objects of different width. They are expected to be used in the field of target identification and medical diagnosis.

Acknowledgements

Our research is funded by The National Key Research and Development Program of China (grant number 2021YFC3340502). We thank the support from the faculty of Nanjing Normal University.

References

[1] Qi,Y.,Yang,Z., Sun,W., Lou, M., Lian,J., Zhao,W., Deng,X. and Ma,Y. (2021) A Comprehensive Overview of Image Enhancement Techniques. Arch. Comp. Met. Eng. 29,583-607.
[2] Lin, S.C.F., Wong, C.Y., Rahman, M.A., Jiang, G., Liu, S., Kwok, N., Shi, H., Yu, Y.-H. and Wu, T. (2015) Image enhancement using the averaging histogram equalization (AVHEQ) approach for contrast improvement and brightness preservation. Com. & Elec. Eng. 46,356-370.
[3] Cho, D. and Bui, T.D. (2014) Fast image enhancement in compressed wavelet domain. Signal Process., 98,295-307.
[4] Liu, T., Zhang, W.and Yan, S.(2015) A novel image enhancement algorithm based on stationary wavelet transform for infrared thermography to the de-bonding defect in solid rocket motors. Mecha. Sys. Sign. Proce. 62-63,366-380.
[5] Khatkar, K. and Kuman, D. (2015) Biomedical Image Enhancement Using Wavelets. Procedia Comp. Sci. 48, 513-517.
[6] Wang, Y., Wang, H.,Yin, C. and Dai, M. (2016) Biologically inspired image enhancement based on Retinex. Neurocomputing, 177,373-384.
[7] Tang, L., Chen, S., Liu, W.and Li, Y. (2011) Improved Retinex Image Enhancement Algorithm. Procedia Environ. Sci. 11,208-212.
[8] Zotin, A. (2018) Fast Algorithm of Image Enhancement based on Multi-Scale Retinex. Procedia Comp. Sci. 131, 6-14.
[9] Jiang, X., Yao, H. and Liu, D. (2018) Nighttime image enhancement based on image decomposition.Sign. Image Video Process.13,189-197.
[10] Cheng, H.D. and Xu, H. (2000) A novel fuzzy logic approach to contrast enhancement. Pattern Recognition. 33, 809-819.
[11] Yu,C.-Y., Lin,H.-Y. and Lin, C.-J.(2021) Image contrast expand enhancement system based on fuzzy theory. Microsystem Tech. 27,1579-1587.
[12] Li,C., Yang,Y., Xiao,L., Li,Y., Zhou,Y. and Zhao,J.(2016) A novel image enhancement method using fuzzy Sure entropy. Neurocomputing.215,196-211.
[13] Selvam, C. and Sundaram, D.(2025) Interval-valued intuitionistic fuzzy generator based low-light enhancement model for referenced image datasets. Artificial Intelligence Review. 58,141.
[14] Jiang, Y., Tong, G., Yin, H. and Xiong, N.(2019) A Pedestrian Detection Method Based on Genetic Algorithm for Optimize XGBoost Training Parameters. IEEE Access. 7, 118310-118321.
[15] Lu, Y., Wu, S., Fang, Z., Xiong, N., Yoon, S. and Park, D. S.(2017) Exploring finger vein based personal authentication for secure IoT.Future Generation Computer Systems. 77, 149-160.
[16] Wan, R., Xiong, N. and The Loc, N. (2018) An energy-efficient sleep scheduling mechanism with similarity measure

for wireless sensor networks. Hum. Cent. Comput. Inf. Sci. 8, 1-22.
[17] Xia, F., Hao, R., Li, J.,Xiong, N., Yang, L. T. and Zhang, Y.(2013) Adaptive GTS allocation in IEEE 802.15.4 for real-time wireless sensor networks. J. Sys. Architect. 59, 1231-1242.
[18] Yao, Y., Xiong, N., Park. J. H., Ma, L. and Liu, J.(2013) Privacy-preserving max/min query in two-tiered wireless sensor networks. Computers & Mathematics with Applications. 65, 1318-1325.
[19] Sobbahi, R. and Tekli, J.(2022) Signal Proce. Comparing deep learning models for low-light natural scene image enhancement and their impact on object detection and classification: Overview, empirical evaluation, and challenges. Image Comm. 109,116848.
[20] Sobbahi,R. and Tekli, J.(2022) Low-Light Homomorphic Filtering Network for integrating image enhancement and classification. Sig. Proce. - Image Comm. 100,116527.
[21] Sun, T., Xu,J., Li, Z. and Wu, Y. (2025) Two Non-Learning Systems for Profile-Extraction in Images Acquired from a near Infrared Camera, Underwater Environment, and Low-Light Condition. Applied Sciences. 15,11289.
[22] Zhou, B., Wang, W., Wang, J., Gu, H. and Wu,Y. (2025) Application of Frequency Domain Filter Banks in Audio Denoising. 2025 8th International Conference on Advanced Electronic Materials, Computers and Software Engineering (AEMCSE).360-364.
[23] Jia,M., Xu, J., Yang, R., Li, Z., Zhang, L. and Wu, Y.(2023) Three filters for the enhancement of the images acquired from fluorescence microscope and weak-light-sources and the image compression. Heliyon. 9,e20191.
[24] Lin, Y., Zhang,L., Xu, J. and Wu, Y. (2025) Three Filters for Enhancing Images Acquired from Blue Fluorescence Imaging, Low Light Condition, and a Near Infrared Camera. International Journal of Epidemiology and Public Health Research. 7(1).
[25] Huang, Y., Yang, R., Geng, X., Li, Z. and Wu, Y.(2023) Two Filters for Acquiring the Profiles from Images Obtained from Weak-Light Background, Fluorescence Microscope, Transmission Electron Microscope, and Near-Infrared Camera. Sensors.23,6207.
[26] Yang, R., Chen, L., Zhang, L., Li,Z.,Lin,Y. and Wu, Y. (2023) Image enhancement via special functions and its application for near infrared imaging. Global Challenges. 7, 2200179.
[27] Wu, J. and Wu,Y. (2025) Two Filters Based on Simple Functions for Extracting Profiles from Images. Advances in Computer, Signals and Systems.9,3.
[28] Li, Z., Yao, S., Xu, J., Wu, Y., Li, C. and He, Z. (2018) Endoscopic near-infrared dental imaging with indocyanine green: a pilot study. Annals of the New York Academy of Sciences. 1421,88-96.
[29] Zhu, J., Shao, X.J., Li, Z., Lin, C.H., Wang, C.W.Q., Jiao, K., Xu, J., Pan, H.X. and Wu, Y. (2022) Synthesis of holmium-oxide nanoparticles for near-infrared imaging and dye-photodegradation. Molecules. 27, 3522.
[30] Li, Z., Li, Y., Lin, Y., Alam, M.Z. and Wu, Y. (2020) Synthesizing Ag+: MgS, Ag+: Nb2S5, Sm3+: Y2S3, Sm3+:Er2S3, and Sm3+:ZrS2 Compound Nanoparticles for Multicolor Fluorescence Imaging of Biotissues.ACS Omega. 5,32868-32876.
[31] Wu, Y., Ou, P., Song, J., Zhang, L., Lin, Y., Song, P. and Xu, J. (2020) Synthesis of praseodymium-and molybdenum-sulfide nanoparticles for dye-photodegradation and near-infrared deep-tissue imaging. Materials Research Express. 7,036203.
[32] Fu, H., Ou, P., Zhu, J., Song, P., Yang, J and Wu, Y.(2019) Enhanced protein adsorption in fibrous substrates treated with zeolitic imidazolate framework-8 (ZIF-8) nanoparticles. ACS Applied Nano Materials. 2, 7626-7636.
[33] Wu,Y., Ou, P., Fronczek, F.R.,Song,J., Lin,Y., Wen,H.M. and Xu, J.(2019) Simultaneous Enhancement of Near-Infrared Emission and Dye Photodegradation in a Racemic Aspartic Acid Compound via Metal-Ion Modification.ACS Omega. 4, 19136-19144.
[34] Wu, Y., Yang,J., Lin,Y., Xu, J.(2019) Synthesis of samarium-based metal organic compound nanoparticles with polychromatic-photoluminescence for bio-tissue fluorescence imaging. Molecules.24,3657.
[35] Wu,Y., Xu, J., Guo,R. (2019) Achieving near-infrared deep tissue imaging via metal organic complex nanoparticles. Photonic Fiber and Crystal Devices: Advances in Materials and Innovations in Device Applications XIII. 11123,143-149.
[36] Wu, Y., Lin,Y., Xu,J.(2019) Synthesis of Ag–Ho, Ag–Sm, Ag–Zn, Ag–Cu, Ag–Cs, Ag–Zr, Ag–Er, Ag–Y and Ag–Co metal organic nanoparticles for UV-Vis-NIR wide-range bio-tissue imaging. Photochemical &Photobiological Sciences.18,1081-1091.
[37] Li, F., Yang, R., Xu, J., Xu, G., Wu, Y. (2024) Detecting N-Phenyl-2-Naphthylamine, L-Arabinose, D-Mannose, L-Phenylalanine, L-Methionine, and D-Trehalose via Photocurrent Measurement.Gels.10,808.